

# High Yield Production of Natural Phenolic Alcohols from Woody Biomass Using a Nickel-Based Catalyst

Jiazhi Chen,<sup>[a]</sup> Fang Lu,<sup>\*[a]</sup> Xiaoqin Si,<sup>[a, b]</sup> Xin Nie,<sup>[a]</sup> Junsheng Chen,<sup>[a]</sup> Rui Lu,<sup>[a, b]</sup> and Jie Xu<sup>\*[a]</sup>

Efficient depolymerization of woody biomass to produce natural phenolic alcohols not only preserves the original structure of lignin, but also makes the depolymerization process atom-efficient. Here, high yield production of natural phenolic alcohols (38.7 wt%) from woody biomass has been achieved using a Ni/C catalyst in a methanol–water co-solvent. The Ni-based catalyst can efficiently etherify the C<sub>α</sub>–OH group in lignin β-O-4 motifs under hydrogen atmosphere, which can break the hydrogen bond between the C<sub>β</sub>–O oxygen and the C<sub>α</sub>–OH

proton to facilitate the C<sub>β</sub>–O cleavage. It was reported that water can also accelerate the etherification of raw lignin with methanol through in situ formation of acid. Our results suggest that breaking the intramolecular hydrogen bonds can accelerate the C<sub>β</sub>–O cleavage, keeping the original structure of lignin unchanged. This work highlights the significance of structure modification in lignin depolymerization and displays a clear potential for the valorization of whole biomass.

## Introduction

The efficient use of natural resources is currently attracting a lot of attentions in both science and technology field.<sup>[1]</sup> Lignin, along with cellulose and hemicellulose, is one of the main constituents of lignocellulosic biomass (40% by energy). It has great potentials to be developed into major industrial raw materials for the production of high quality liquid fuel and pharmacological applications.<sup>[2]</sup> Three monolignols, *p*-coumaryl, coniferyl and sinapyl alcohols are major components of lignin, and are randomly bonded through different C–O–C and C–C linkages to form cross-linked amorphous copolymer structure.<sup>[3]</sup> These natural phenolic alcohols have broadly biological and pharmacological activities and can be utilized in the pharmacological fields. They possess a hydroxyl group at the C<sub>γ</sub> position and a phenolic hydroxyl group per phenolic propane unit, which make them possible for the production of polyurethanes and polyesters.<sup>[4]</sup> Unfortunately, lots of lignin depolymerization methods remove too much oxygen and/or disrupt the aromatic ring to produce low value chemicals.<sup>[5]</sup> Therefore, one of the great challenges remaining for efficiently depolymerizing lignin is to produce natural phenolic alcohols from lignocellulose that not only preserves the original structure of

lignin, but also makes the depolymerization process atom-efficient.

Among hydrolysis, pyrolysis, oxidation, and hydrogenation, hydrogenation has been considered as a promising method to efficiently depolymerize lignin.<sup>[6]</sup> The hydrogenation of lignin model compounds has already made great advances<sup>[7]</sup> and a few groups have reported the hydrogenation of raw lignocellulose materials recently (summarized in Table S1 in the Supporting Information). Noble metal-based catalysts, such as Pd, Pt, and Ru, have been reported for the directly reductive cleavage of C–O ether bonds in lignin.<sup>[8]</sup> The W<sub>2</sub>C catalyst, which has noble-metal-like properties, has been reported to successfully hydrogenate birch sawdust to guaiacyl and syringyl derivatives with the help of a Ni-based catalyst.<sup>[9]</sup>

In our previous work, we demonstrated that non-noble metal Ni-based catalysts can efficiently depolymerize birch sawdust without the use of a co-catalyst, using methanol to provide an active hydrogen species.<sup>[10]</sup> Abu-Omar et al.<sup>[11]</sup> also reported that Ni/C is a good catalyst to efficiently depolymerize lignocellulose; however, phenolic propanes were obtained as the main products, in which the hydroxyl group at the C<sub>γ</sub> position was removed. Therefore, it still remains a challenge to efficiently hydrogenate raw woody biomass to natural phenolic alcohols using Ni-based catalysts.

Herein, the aim of this work is to develop a strategy for the high yield production of natural phenolic alcohols from woody biomass using Ni catalysts. The strategy is to selectively modify the C<sub>α</sub>–OH group through an etherification process. Breaking the hydrogen bond between the C<sub>α</sub>–OH hydrogen and C<sub>β</sub>–O oxygen can facilitate the C<sub>β</sub>–O cleavage. It was reported that Ni can be used as a catalyst for etherification of lignin β-O-4 model compounds and methanol under hydrogen atmosphere to break the hydrogen bond. In addition, water has been reported to accelerate the etherification of the

[a] J. Chen, Prof. Dr. F. Lu, X. Si, X. Nie, J. Chen, R. Lu, Prof. Dr. J. Xu  
State Key Laboratory of Catalysis  
Dalian National Laboratory for Clean Energy  
Dalian Institute of Chemical Physics  
Chinese Academy of Sciences  
457 Zhongshan Road, Dalian 116023 (China)  
E-mail: lufang@dicp.ac.cn  
xujie@dicp.ac.cn

[b] X. Si, R. Lu  
Chinese Academy of Sciences  
Beijing 100049 (China)

Supporting Information for this article can be found under:  
<http://dx.doi.org/10.1002/cssc.201601273>.

C<sub>α</sub>-OH in beech sawdust through in situ formation of acid catalyst.

## Results and Discussion

### Characterization of hydrogen bonding in β-O-4 model compounds

To investigate the nature of the hydrogen bond in lignin β-O-4 motifs, variable-temperature <sup>1</sup>H NMR experiments were performed. Guaiacylglycerol-β-guaiacyl ether (GGGE) and guaiacylglycerol-α-methyl-β-guaiacyl ether (GGMGE) were chosen as β-O-4 model compounds. Figure 1a shows the partial variable-temperature <sup>1</sup>H NMR spectra of the C<sub>α</sub>-OH proton of GGGE in CDCl<sub>3</sub> in the range of 298–328 K. The chemical shift of the C<sub>α</sub>-OH proton moved from 3.62 ppm to 3.50 ppm with increasing the temperature. For GGMGE, the C<sub>α</sub>-OH proton was removed and resulted in a C<sub>α</sub>-OCH<sub>3</sub> group (Figure 1b). A slope value from the linear fits of lnδ versus 1/T was used for the distinction of the hydrogen bond according to our previously proposed Arrhenius-like equation. The C<sub>α</sub>-OH proton of GGGE shows a slope value of 113.0 (inset in Figure 1c), suggesting that it may involve an intramolecular hydrogen bond. On the other hand, the C<sub>α</sub>-OH proton has a coupling constant (<sup>3</sup>J<sub>HCOH</sub>) of 1.8 Hz (inset in Figure 1c), which deviates significantly from

5.5 Hz.<sup>[12]</sup> It indicates the restricted rotation around the C<sub>α</sub>-O bond owing to the presence of the hydrogen bonding. Therefore, above results suggest that an intramolecular hydrogen bond exists in GGGE, and the intramolecular hydrogen bond in GGMGE disappears because the C<sub>α</sub>-OH proton was replaced by methyl group.

Density functional theory (DFT) calculations were employed to understand the intramolecular hydrogen bond in GGGE using the hybrid meta-GGA M062X<sup>[13]</sup> functional and 6-31g(2d,2p) basis set with the Gaussian 09 program. The optimized geometry of GGGE demonstrated that the C<sub>α</sub>-OH proton participated in intramolecular hydrogen bonding to the C<sub>β</sub>-O oxygen (OH<sub>α</sub>...O<sub>β</sub>, 2.37 Å) and the oxygen of the aromatic methoxy group (OH<sub>α</sub>...O<sub>methoxy</sub>, 2.19 Å) (Figure 1d), which is consistent with the geometry observed in the crystal structures of lignin β-O-4 models.<sup>[14]</sup> The computational results also predicted the C<sub>β</sub>-O bond of GGGE to have a bond dissociation enthalpy (BDE) value of 289 kJ mol<sup>-1</sup>, while the C<sub>β</sub>-O BDE value of GGMGE is 20 kJ mol<sup>-1</sup> lower (Figure 1d). Kim et al.<sup>[15]</sup> and Younker et al.<sup>[16]</sup> reported that disruption of intramolecular hydrogen bonds can potentially reduce the C<sub>β</sub>-O BDE. These results suggest that methylation of the C<sub>α</sub>-OH group in β-O-4 structure breaks intramolecular hydrogen bonds and might weaken the C<sub>β</sub>-O bond.

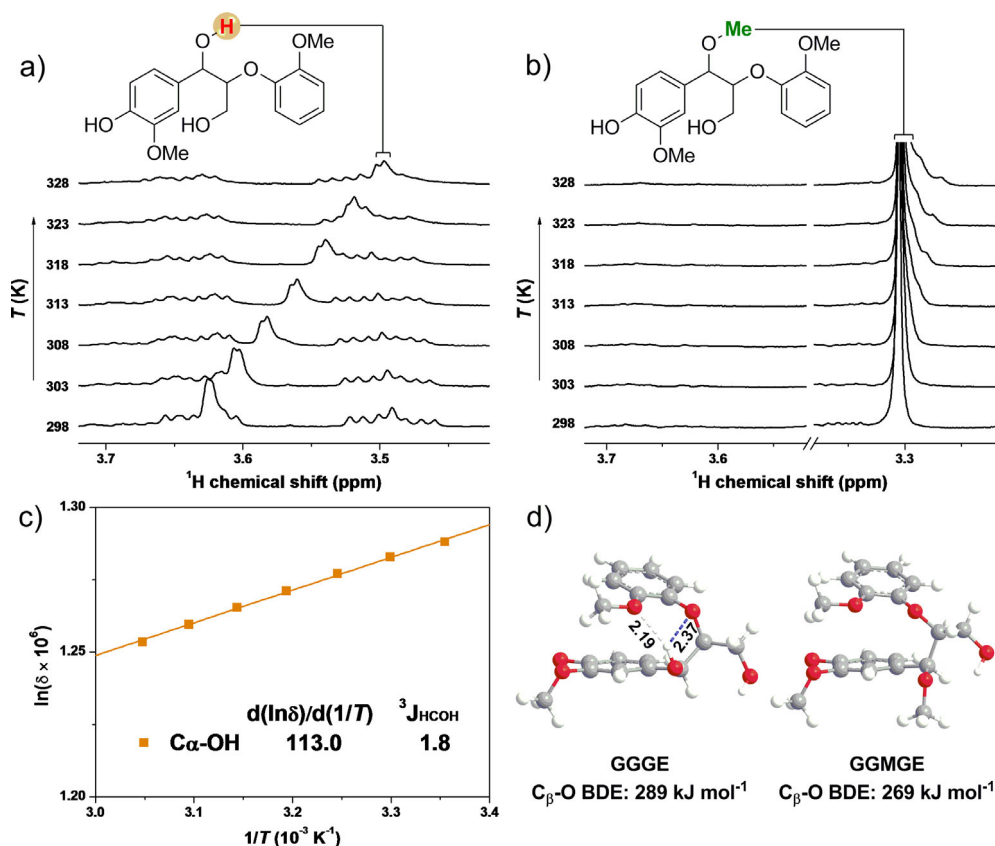


**Figure 1.** Partial variable-temperature <sup>1</sup>H NMR spectra of a) the C<sub>α</sub>-OH proton of GGGE and b) the C<sub>α</sub>-OCH<sub>3</sub> proton of GGMGE in CDCl<sub>3</sub>, c) Plots and linear fits ( $R_2 > 0.999$ ) of lnδ of the C<sub>α</sub>-OH proton versus 1/T for GGGE, the inset illustrates the slope value d(lnδ)/d(1/T) and the coupling constant <sup>3</sup>J<sub>HCOH</sub>, d) Optimized geometries of GGGE with hydrogen-bond lengths in Å and GGMGE, and their computational C<sub>β</sub>-O BDEs.

### Comparison of C<sub>β</sub>-O bond cleavage activity using different β-O-4 model compounds with and without hydrogen bonding

To compare the C<sub>β</sub>-O cleavage reactivity between GGGE and GGMGE, hydrogenolysis reactions were performed in polar aprotic solvent with a Ni/C catalyst. As shown in Table 1, guaiacol and guaiacylpropanol (GPol) were obtained as main products, and eugenol, isoeugenol, and 4-propylguaiacol derived from GPol were also identified. Considering one substrate molecule can generate two monomeric products, each monomer yield is defined as 50% of the molar ratio of this monomer to the substrate. The total phenolic monomer yield provided an indication of the C<sub>β</sub>-O cleavage reactivity. Entries 1 and 2 in Table 1 compare the results of GGGE and GGMGE in dioxane for 1 h. GGGE exhibited a total phenolic monomer yield of 8.3% with a conversion of 12.5% (Table 1, entry 1), whereas GGMGE showed 3× higher yield towards monomers (26.5%) with higher conversion (39.5%) at the same conditions (Table 1, entry 2), indicating a higher C<sub>β</sub>-O hydrogenolysis reactivity. Prolonging the reaction time to 2 h resulted in 15.5% monomer yield from GGGE and 41.8% monomer yield from GGMGE, respectively (Table 1, entries 3 and 4). When the reactions were carried out in tetrahydrofuran (THF) for 1 h, GGGE gave 7.1% phenolic monomers. The phenolic monomer yield reached 26.3% from GGMGE, which is approximately 3× higher than that from GGGE (Table 1, entries 5 and 6). In addition, a control experiment without catalyst was demonstrated in entry 7. The GGMGE conversion was 13.3%, but the total monomer yield was only 1.1%. These results demonstrate that the C<sub>β</sub>-O bond in the C<sub>α</sub>-OH etherified β-O-4 model compound GGMGE is easier to be cleaved than that in GGGE.

### Effect of metal catalysts for in situ etherification method

To put this structural etherification strategy into practice, in situ formation of the active C<sub>α</sub>-OH etherified intermediate coupled with hydrogenolysis was developed for efficient C<sub>β</sub>-O bond cleavage. By using methanol as etherification reagent and solvent, we firstly tested several reduced metal-based catalysts for the selective etherification of the C<sub>α</sub>-OH group in GGGE (Table 2). Ru/C provided a C<sub>α</sub>-OH methylated product GGMGE yield of 1.4% with a conversion of 12.3% under 20 bar H<sub>2</sub>, as well as Pd/C (Table 2, entries 1 and 2). When Ni-based catalysts were employed, the GGMGE yield dramatically increased (Table 2, entries 3–6). Ni/C exhibited 98.6% conversion of GGGE and 72.8% yield of GGMGE, which is the excellent one among those tested catalysts. As a control, the reaction was conducted using Ni/C under 20 bar N<sub>2</sub>. Only 3.9% yield of GGMGE was obtained (Table 2, entry 7). It is known that reduced nickel oxide is effective for converting aliphatic alcohol to ether in presence of H<sub>2</sub>.<sup>[17]</sup> Without any catalyst in H<sub>2</sub> atmosphere, GGMGE yielded 3.2% (Table 2, entry 8). These results suggested that the catalytic system with Ni/C and H<sub>2</sub> was effective for GGGE etherification.

### Cascade etherification–hydrogenolysis reactions of model compounds

A higher reaction temperature was used to perform the cascade etherification–hydrogenolysis reactions of GGGE in methanol using Ni/C as catalysts. Representative chromatograms of reaction products were demonstrated in Figure S1. Guaiacol and GPol were identified as main products. The reaction data were shown in Table 3. At the reaction time of 2 min, 86.9% conversion of GGGE generated 61.2% yield of GGMGE and 16.8% yield of total phenolic monomers (Table 3, entry 1). As the reaction proceeded, the intermediate GGMGE slightly increased to a yield of 64.1% and then decreased to 9.1%.

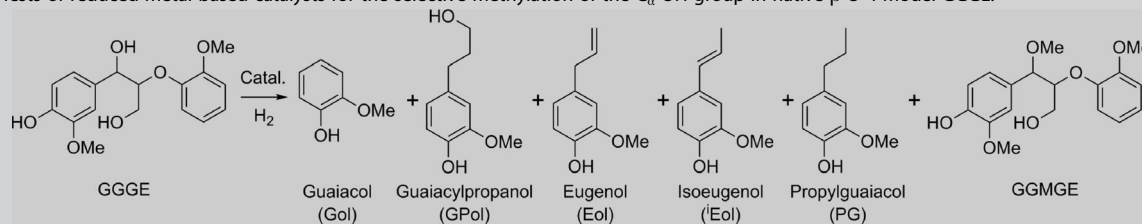
**Table 1.** C<sub>β</sub>-O cleavage of lignin β-O-4 model and C<sub>α</sub>-OH methylated β-O-4 model compounds by Ni-catalyzed hydrogenolysis.<sup>[a]</sup>

R=H: GGGE;  
R=Me: GGMGE

Guaiacol (Gol)    Guaiacylpropanol (GPol)    Eugenol (Eol)    Isoeugenol (iEol)    Propylguaiacol (PG)

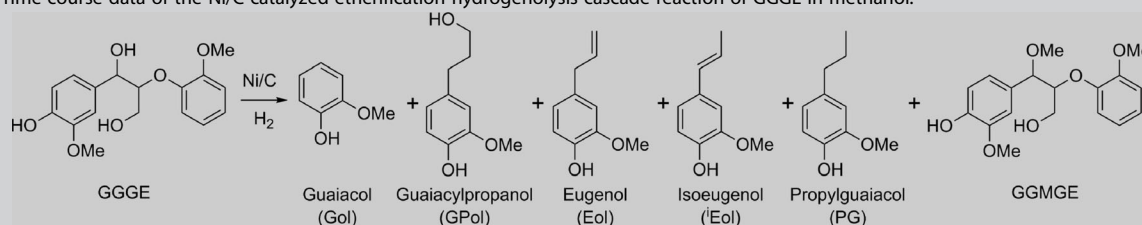
Entry	Substrate	Conv. [%]	Phenolic monomer yield [%]					total
			Gol	GPol	Eol	iEol	PG	
1	GGGE	12.5	3.2	4.2	0.5	0.0	0.4	8.3
2	GGMGE	39.5	11.4	1.6	0.1	11.1	2.3	26.5
3 <sup>[b]</sup>	GGGE	26.8	6.4	7.7	0.8	0.0	0.6	15.5
4 <sup>[b]</sup>	GGMGE	71.9	19.3	2.0	0.8	14.2	5.5	41.8
5 <sup>[c]</sup>	GGGE	15.7	2.4	2.7	1.6	0.0	0.4	7.1
6 <sup>[c]</sup>	GGMGE	52.6	12.2	3.8	0.9	9.4	0.0	26.3
7 <sup>[d]</sup>	GGMGE	13.3	0.4	0.1	0.3	0.3	0.0	1.1

[a] Reaction conditions: substrate (0.1 g), Ni/C (0.025 g, 10 wt % Ni loading), dioxane (10 mL), 150 °C, 20 bar H<sub>2</sub>, 1 h. [b] 2 h. [c] THF (10 mL). [d] THF (10 mL) without any catalyst.

**Table 2.** Tests of reduced metal-based catalysts for the selective methylation of the C<sub>α</sub>-OH group in native β-O-4 model GGGE.<sup>[a]</sup>

Entry	Catalyst	Conv. [%]	Phenolic product yield [%]					GGMGE
			Gol	GPol	Eol	iEol	PG	
1	Ru/C	12.3	2.9	2.2	1.4	0.2	0.9	1.4
2	Pd/C	12.8	3.7	3.1	1.4	0.2	0.8	1.4
3	Ni/C	98.6	9.2	7.4	0.2	0.3	0.5	72.8
4	Ni/Al <sub>2</sub> O <sub>3</sub>	96.5	4.0	3.1	0.5	0.1	0.3	59.0
5	Ni/ZrO <sub>2</sub>	68.4	1.1	0.9	0.1	0.9	0.6	56.3
6	Ni/SiO <sub>2</sub>	37.1	1.9	1.3	1.2	0.0	0.0	14.1
7 <sup>[b]</sup>	Ni/C	19.6	1.9	2.0	0.7	0.2	3.5	3.9
8	Blank	5.2	0.2	0.2	0.0	0.3	0.0	3.2

[a] Reaction conditions: GGGE (0.1 g), catalyst (0.025 g), methanol (10 mL), 120 °C, 20 bar H<sub>2</sub>, 2 h. [b] 20 bar N<sub>2</sub>.

**Table 3.** Time course data of the Ni/C-catalyzed etherification-hydrogenolysis cascade reaction of GGGE in methanol.<sup>[a]</sup>

Entry	t [min]	Conv. [%]	Phenolic product yield [%]					total	GGMGE
			Gol	GPol	Eol	iEol	PG		
1	2	89.6	7.2	5.8	2.8	0.5	0.5	16.8	61.2
2	10	96.7	10.7	8.6	2.8	0.2	1.5	23.9	64.1
3	20	98.5	14.4	11.8	3.0	0.2	1.1	30.8	58.2
4	60	100.0	24.9	20.7	2.9	0.2	1.4	50.5	39.6
5	120	100.0	29.1	24.0	2.7	0.0	1.6	58.3	29.9
6	240	100.0	36.0	29.1	2.8	0.2	1.5	70.2	19.0
7	360	100.0	39.0	33.3	2.7	0.2	1.2	76.6	14.2
8	480	100.0	41.8	35.8	2.6	0.3	1.3	82.0	9.1

[a] Reaction conditions: GGGE (0.1 g), Ni/C (0.025 g, 10 wt% Ni loading), methanol (10 mL), 150 °C, 20 bar H<sub>2</sub>.

Meanwhile, the monomers increased gradually to a yield of 82.0% within the overall tested time, which included 35.8% of GPol (phenolic alcohols) and 41.8% of guaiacol in yield (Table 3, entries 2–8). These results revealed that GGGE converted quickly into the C<sub>α</sub>-OH etherified intermediate GGMGE and then decomposed with the Ni/C and H<sub>2</sub> catalytic system. Optimizing the conditions at 180 °C for 2 h achieved completed conversion of GGGE with 36.1% of GPol and 46.4% of guaiacol (Figure S2).

### Water accelerates the etherification process of sawdust

Besides Ni-based catalysts, water is also important during the etherification of real lignin. Methanosolv lignin treated in dif-

ferent water content was isolated from Beech sawdust (*Fagus sylvatica*) by an autocatalytic organosolv process. Dioxasolv lignin was also performed using the same procedure as a control lignin. The lignin structure was determined by 2D HSQC NMR techniques following reported procedures.<sup>[18]</sup> Three main linkages, (β-O-4, A), (β-5, B), and (β-β, C), were observed in all lignin fractions (Figure 2a–d) and semi-quantified using the guaiacyl G<sub>2</sub> and syringyl S<sub>2,6</sub> cross-peaks as the reference.<sup>[19]</sup> Semi-quantification provided that the linkages per 100 C<sub>9</sub> units were 51.9 (A), 4.2 (B), and 8.0 (C) and the S/G unit ratio was 3.0:1.0 in the dioxasolv lignin (Figure 2a). For methanosolv lignins, HSQC analysis revealed the appearance of the C<sub>α</sub>-OH methylated β-O-4 (A<sup>Me</sup>) signals in green-coded cross peaks, of which the C<sub>α</sub>-H coupling was identified at δ<sub>C</sub>/δ<sub>H</sub> 82.3:4.44 and

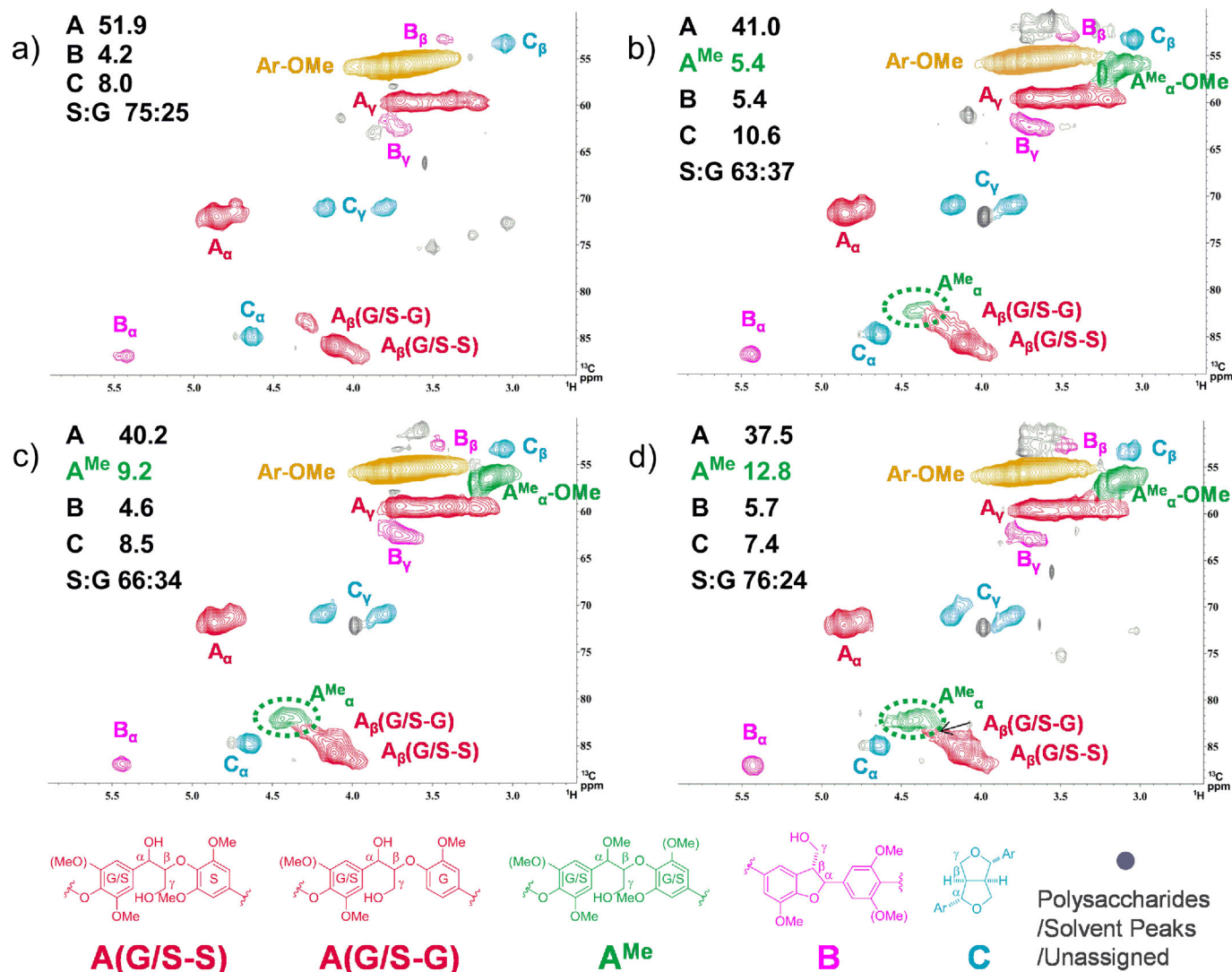


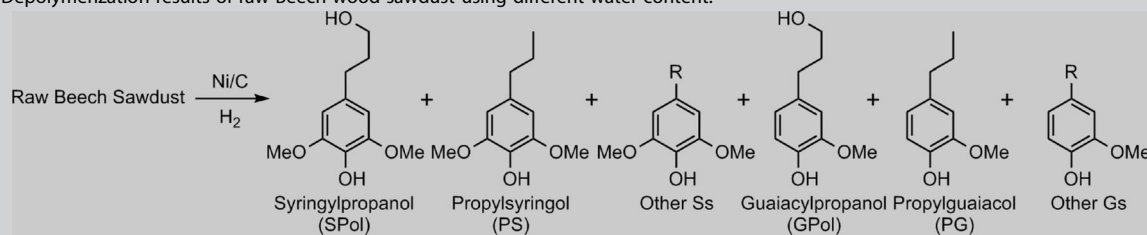
**Figure 2.** Partial 2D HSQC NMR spectra of lignin fractions isolated from Beech wood sawdust by an autocatalytic organosolv process in a) 60% aqueous dioxane, b) methanol, c) 80% aqueous methanol, and d) 60% aqueous methanol. Amounts of  $\beta$ -O-4 (A),  $C_{\alpha}$ -methoxylated  $\beta$ -O-4 ( $A^{Me}$ ),  $\beta$ -5 (B), and  $\beta$ - $\beta$  (C) linkages relative to 100  $C_{\alpha}$  units and S/G ratios are given.

the methyl group in  $A^{Me}$  was observed at  $\delta_C/\delta_H$  56.5:3.15 (Figure 2b–d). The methanosolv lignin extracted from pure methanol retained 46.4% of A including 5.4% of  $A^{Me}$  (Figure 2b). When water was added into the methanosolv process, the content of  $A^{Me}$  was increased. The methanosolv lignin isolated from 80% aqueous methanol showed 49.4% of A, including 9.2% of  $A^{Me}$  (Figure 2c). And the  $A^{Me}$  content in the methanosolv lignin from 60% aqueous methanol further increased to 12.8% (Figure 2d). According to the mechanism discussed previously, this is expected that water could increase the releasing of acetic acid from wood sawdust and the acidic catalyst would accelerate the nucleophilic substitution at  $C_{\alpha}$  position with methanol.<sup>[20]</sup> NMR results demonstrated that the linkages and total  $\beta$ -O-4 contents in methanosolv lignin were quite similar to the dioxanosolv lignin except for the  $C_{\alpha}$ -OH methylated  $\beta$ -O-4 substructure.

### Hydrogenolysis of raw Beech sawdust in aqueous methanol

Based on the above results, the etherification-hydrogenolysis method was applied in the depolymerization of raw Beech hardwood sawdust. As shown in Table 4, two natural phenolic alcohols syringylpropanol (SPol) and GPol were obtained as main products. Besides,  $C_1$ – $C_3$  alkylsyringols and alkylguaiacols, like propylsyringol (PS) and propylguaiacol (PG), were identified as other phenolic monomers (see Table S2 for more details). Entries 1–6 compare the results for reactions in aqueous methanol and pure methanol. In 60% aqueous methanol, hydrogenolysis of raw Beech sawdust yielded 51.4 wt% phenolic monomers with a total selectivity of 75.3% towards SPol and GPol (Table 4, entry 1). The yield of SPol and GPol was 28.9 and 9.8 wt%, respectively. The yield of SPol and GPol was slightly dropped to 26.6 and 9.0 wt% when 80% aqueous methanol was used as solvent (Table 4, entry 2). In comparison, the reac-

**Table 4.** Depolymerization results of raw Beech wood sawdust using different water content.<sup>[a]</sup>



Entry	Solvent	Phenolic monomer yield [wt%] <sup>[c]</sup>						total	SPol + GPol select. [%]
		SPol	PS	other Ss	GPol	PG	other Gs		
1	MeOH/H <sub>2</sub> O (6:4, v/v)	28.9	7.9	2.0	9.8	0.7	2.1	51.4	75.3
2	MeOH/H <sub>2</sub> O (8:2, v/v)	26.6	6.8	1.3	9.0	1.2	0.8	45.7	77.9
3	MeOH	18.5	7.7	2.2	7.5	2.6	0.8	39.3	66.2
4 <sup>[b]</sup>	MeOH/H <sub>2</sub> O (6:4, v/v)	19.2	7.6	5.1	7.7	0.9	3.7	44.2	60.9
5 <sup>[b]</sup>	MeOH/H <sub>2</sub> O (8:2, v/v)	23.3	5.0	1.6	8.8	0.9	0.9	40.5	79.3
6 <sup>[b]</sup>	MeOH	18.3	2.7	1.8	6.9	1.0	0.6	31.3	80.5
7	dioxane	8.1	0.9	0.3	4.2	0.3	0.5	14.3	86.0

[a] Reaction conditions: Beech sawdust (1.0 g), Ni/C (0.10 g, 10 wt% Ni loading), solvent (20 mL), 200 °C, 20 bar H<sub>2</sub>, 5 h. [b] 0.05 g Ni/C. [c] Phenolic monomer yield calculated based on the Klason lignin content in raw Beech sawdust. The Klason lignin in raw Beech sawdust is 21.0 wt%. Other Ss contain 3-methoxypropylsyringol, 4-propenylsyringol, 4-ethylsyringol, 4-methylsyringol, and syringol; Other Gs contain 3-methoxypropylguaiacol, 4-propenylguaiacol, 4-ethylguaiacol, 4-methylguaiacol, and guaiacol.

tion in pure methanol gave a SPol yield of 18.5 wt% and a GPol yield of 7.5 wt% (Table 4, entry 3). Similar catalytic performances were observed in the reactions using half amounts of Ni/C catalysts (Table 4, entries 4–6). Next, another reaction was compared in dioxane solvent, yielding only 8.1 wt% of SPol and 4.2 wt% of GPol (Table 4, entry 7). The much higher phenolic alcohol yield from sawdust in aqueous methanol is likely owing to an efficient etherification–hydrogenolysis approach by Ni/C and H<sub>2</sub> catalytic systems and the mixed water during methanosolv lignin fractionation.

## Conclusions

High yield production of natural phenolic alcohols (38.7 wt%) from woody biomass has been achieved using a Ni/C catalyst in a methanol–water co-solvent. The NMR results and density functional theory (DFT) calculations suggested that replacement of the C<sub>α</sub>–OH proton in GGGE with a methyl group breaks intramolecular hydrogen bonds and weakens the C<sub>β</sub>–O bond. Using this Ni-based catalyst, we can efficiently etherify the C<sub>α</sub>–OH group in lignin, which can break the hydrogen bond (OH<sub>α</sub>⋯O<sub>β</sub>) to facilitate the C<sub>β</sub>–O cleavage. 2D HSQC NMR analysis shows that water can also accelerate the etherification of raw lignin with methanol through in situ formation of acid catalyst. The above results show that breaking the intramolecular hydrogen bonds accelerate the C<sub>β</sub>–O cleavage, maintaining the original structure of lignin. This work highlights the significance of structure modification in lignin depolymerization and displays clear potential for the valorization of whole biomass.

## Experimental Section

To determine the lignin content in Beech sawdust, the T222 om-02 TAPPI standard method was used. Briefly, Beech (*Fagus sylvatica*) sawdust was firstly treated with an ethanol/benzene mixture (1:2, v/v) in a Soxhlet extractor for 12 h to remove resin, wax, and fat. Then, the sawdust was washed with ethanol, dried at 100 °C for 4 h, and weighted. The dried powder (1.00 g) was placed in a flask and mixed gradually with 72 wt% H<sub>2</sub>SO<sub>4</sub> (15 mL) in an ice bath under stirring. Then, the flask was placed in a 20 °C bath for 2 h. After that, the mixture was diluted to 3 wt% H<sub>2</sub>SO<sub>4</sub> solution, refluxed for 4 h, and then cooled down to room temperature. The solution was filtered, and the solid residue was washed with water until it was neutral. The solid was collected, dried under vacuum (40 °C for 2 days), and weighted (0.2132 g). The Klason lignin percentage was 21.0 wt% based on raw Beech sawdust.

**Characterization of lignin structure:** To characterize hydrogen bonds in β-O-4 model compounds, variable-temperature <sup>1</sup>H NMR experiments were performed. Before measurement, the samples were purified by vacuum freeze drying in liquid nitrogen overnight and then dissolved in dried CDCl<sub>3</sub> (5 mm). The NMR samples were kept for 5 min at each given temperature before acquiring <sup>1</sup>H NMR data. Temperature coefficients were measured over a range of 298 to 328 K. All chemical shifts were calibrated by setting the internal reference (tetramethylsilane) to 0 ppm. 32 000 data points were acquired over 6009.6 Hz spectral width (acquisition time 2.7263 s) using 32 scans and 1 s relaxation delay. The error in <sup>1</sup>H chemical shifts was ±0.001 ppm at a given temperature.

2D <sup>1</sup>H, <sup>13</sup>C HSQC NMR spectra were used to identify lignin structure. The central DMSO solvent peak (δ<sub>C</sub>/δ<sub>H</sub> 39.52:2.49) was used for shift correction. The NMR sample consisted of 40 mg of lignin dissolved in 0.5 mL of [D<sub>6</sub>]DMSO. The HSQC measurement was performed using the standard Bruker pulse sequence hsqcetgpsi.2. The spectral width of 10.3 and 165 ppm (receiver gain: 208) was acquired in the F2 and F1 dimension, respectively. Other parameters for data acquisition included an acquisition time of 130 ms,

a relaxation delay time of 1.5 s, 24 scans, and 1024 data points. The spectra were processed using squared cosine bell in both dimensions. Volume integration of cross-peaks in the HSQC spectra was carried out using MestReNova software. Semi-quantification of the ratios of lignin linkages and aromatic units was calculated following the reported method,<sup>[19]</sup> in which the integrals of  $S_{2,6}$  signals from syringyl units and  $G_2$  signals from guaiacyl units were used as the internal reference (100  $C_9$  units):  $C_9$  units (100) =  $0.5(S_{2,6} + S'_{2,6} + S_{condensed}) + G_2$ .

All calculations presented were accomplished using the DFT method with hybrid meta-GGA M062X<sup>[13]</sup> functional and 6-31g(2d,2p) basis set by Gaussian 09 program.<sup>[21]</sup> These structures were optimized without constraints. At the optimized structures, vibrational frequencies were analyzed to confirm that the structures were at the minima corresponding to the local minima (without imaginary frequency). The zero-point energies and the thermally corrected enthalpies at 298 K were obtained during the frequency analysis. The BDE was calculated as the difference of the sum of the zero-point corrected enthalpies of the parent molecule and the thermally corrected enthalpies of the unimolecular dissociation products.<sup>[15]</sup>

**Catalyst preparation:** Metal-based catalysts were prepared using an incipient-wetness impregnation method and activated by reducing in hydrogen. Typically, supports were added into the aqueous metal salt solution. After ultrasonic dispersion, the slurry was kept at room temperature for 24 h and then dried at 110 °C overnight. Prior to each reaction, the catalysts were activated in a flow of  $H_2$  at 450 °C for Ni-based catalyst, 350 °C for Ru-based catalyst, and 250 °C for Pd-based catalyst, respectively. In particular, activated charcoal support was treated in the nitric acid solution (38 wt%) at 80 °C for 3 h before use.

**Catalytic depolymerization of  $\beta$ -O-4 model compounds:** In a typical catalytic hydrogenolysis experiment of  $\beta$ -O-4 model compounds, 0.1 g of substrate, 10 mL of solvent, and 0.025 g of catalyst were loaded into a 50 mL autoclave (T316 Stainless Steel, ASME SA-479, Parr Instrument). The autoclave was sealed, purged with  $H_2$  to expel air (repeated 5 times), and pressurized with 20 bar  $H_2$  at room temperature. Then the mixture was heated to the desired temperature within 20 min under stirring at a speed of 1000 rpm. After reaction, the autoclave was cooled in an ice-water bath and depressurized at room temperature. The mixture was filtrated to remove the catalyst and filtrate was collected for analysis. Liquid products were identified by GC-MS and HPLC-MS/MS, and the quantification was performed on a Waters e2695 HPLC system equipped with 2489 UV/Vis detector at 272 nm. The products were separated using a C18 column (Agilent ZORBAX extend-C18 column, 4.6 mm  $\times$  150 mm, 5  $\mu$ m) and acetonitrile/water as the mobile phase. A non-linear gradient elution with a flow rate of 1.0 mL min<sup>-1</sup> was used as follows: 25  $\rightarrow$  22%  $CH_3CN$  over 10 min, 22%  $CH_3CN$  for 5 min, 22  $\rightarrow$  60%  $CH_3CN$  over 5 min, 60%  $CH_3CN$  for 2 min, 60  $\rightarrow$  100%  $CH_3CN$  over 1 min, 100%  $CH_3CN$  for 5 min, return to initial conditions over 2 min and re-equilibrate for 5 min. The column was maintained at 30 °C. Products were quantified by using a standard calibration curve in HPLC/UV. Conversion and yield were calculated using the following equations:

$$\text{Conversion} = \left( 1 - \frac{\text{moles of substrate}}{\text{moles of substrate loaded}} \right) \times 100\%$$

$$\text{Yield} = \left( \frac{\text{moles of product} \times \text{number of } C_6 \text{ rings}}{\text{moles of substrate loaded} \times 2} \right) \times 100\%$$

**Catalytic depolymerization of real lignin:** Typically, raw Beech sawdust (100 mesh, 1.0 g), solvent (20 mL), and Ni/C catalyst were placed in a 50 mL autoclave. The reactor was sealed, purged with  $H_2$  to expel air and filled with 20 bar  $H_2$  at room temperature. The reaction was conducted at the desired temperature at a stirring speed of 1000 rpm. After reaction, the autoclave was cooled in an ice-water bath. To analyze the phenolic monomers, a weighed amount of external standard (*n*-decane) was added into the mixture and a sample was filtrated and collected for gas chromatograph (GC)-flame ionization detector (FID) and GC-MS analysis. Phenolic monomers were identified by matching of their retention times to authentic standard samples and through the use of exact mass from GC-MS spectra in the context of expected products. The monomer yield was calculated using the following equation:

$$\text{Yield}_x \text{ (wt \%)} = \left( \frac{\text{mass of } x \text{ monomer}}{\text{mass of Klason lignin in sawdust}} \right) \times 100\%$$

## Acknowledgements

This work was financially supported by the National Natural Science Foundation of China (91545102, 21473188, 21233008).

**Keywords:** carbon-oxygen bond cleavage · etherification · heterogeneous catalysis · hydrogen bond · lignin

- [1] a) C. O. Tuck, E. Perez, I. T. Horvath, R. A. Sheldon, M. Poliakoff, *Science* **2012**, *337*, 695–699; b) G. W. Huber, S. Iborra, A. Corma, *Chem. Rev.* **2006**, *106*, 4044–4098; c) P. N. R. Vennestrom, C. M. Osmundsen, C. H. Christensen, E. Taarning, *Angew. Chem. Int. Ed.* **2011**, *50*, 10502–10509; *Angew. Chem.* **2011**, *123*, 10686–10694.
- [2] a) A. J. Ragauskas, G. T. Beckham, M. J. Biddy, R. Chandra, F. Chen, M. F. Davis, B. H. Davison, R. A. Dixon, P. Gilna, M. Keller, P. Langan, A. K. Naskar, J. N. Saddler, T. J. Tschaplinski, G. A. Tuskan, C. E. Wyman, *Science* **2014**, *344*, 1246843; b) J. E. Holladay, J. F. White, J. J. Bozell, D. Johnson, *Top Value-added Chemicals from Biomass Volume II-Results of Screening for Potential Candidates from Biorefinery Lignins*, U.S. Department of Energy (DOE) by PNNL: Richland, WA, **2007**, pp. 16–30; c) P. C. A. Bruijninx, B. M. Weckhuysen, *Nat. Chem.* **2014**, *6*, 1035–1036.
- [3] J. Zakzeski, P. C. A. Bruijninx, A. L. Jongerius, B. M. Weckhuysen, *Chem. Rev.* **2010**, *110*, 3552–3599.
- [4] a) M. Mastihubová, M. Polakova, *Beilstein J. Org. Chem.* **2016**, *12*, 524–530; b) I. Delidovich, P. J. C. Hausoul, L. Deng, R. Pfitzenreuter, M. Rose, R. Palkovits, *Chem. Rev.* **2016**, *116*, 1540–1599.
- [5] a) X. Y. Wang, R. Rinaldi, *Angew. Chem. Int. Ed.* **2013**, *52*, 11499–11503; *Angew. Chem.* **2013**, *125*, 11713–11717; b) R. Ma, W. Y. Hao, X. L. Ma, Y. Tian, Y. D. Li, *Angew. Chem. Int. Ed.* **2014**, *53*, 7310–7315; *Angew. Chem.* **2014**, *126*, 7438–7443; c) Q. N. Xia, Z. J. Chen, Y. Shao, X. Q. Gong, H. F. Wang, X. H. Liu, S. F. Parker, X. Han, S. H. Yang, Y. Q. Wang, *Nat. Commun.* **2016**, DOI: 10.1038/ncomms11162; d) J. S. Luterbacher, A. Azarpira, A. H. Motagamwala, F. Lu, J. Ralph, J. A. Dumesic, *Energy Environ. Sci.* **2015**, *8*, 2657–2663.
- [6] a) C. Xu, R. A. Arancon, J. Labidi, R. Luque, *Chem. Soc. Rev.* **2014**, *43*, 7485–7500; b) C. Li, X. Zhao, A. Wang, G. W. Huber, T. Zhang, *Chem. Rev.* **2015**, *115*, 11559–11624.
- [7] M. Zaheer, R. Kempe, *ACS Catal.* **2015**, *5*, 1675–1684.
- [8] a) N. Yan, C. Zhao, P. J. Dyson, C. Wang, L. T. Liu, Y. Kou, *ChemSusChem* **2008**, *1*, 626–629; b) T. Parsell, S. Yohe, J. Degenstein, T. Jarrell, I. Klein, E. Gencer, B. Hewetson, M. Hurt, J. I. Kim, H. Choudhari, B. Saha, R. Meilan, N. Mosier, F. Ribeiro, W. N. Delgass, C. Chapple, H. I. Kenttämäa, R. Agrawal, M. M. Abu-Omar, *Green Chem.* **2015**, *17*, 1492–1499; c) S. Van den Bosch, W. Schutyser, R. Vanholme, T. Driessen, S. F. Koelewijn, T. Renders, B. De Meester, W. J. J. Huijgen, W. Dehaen, C. M. Courtin, B. Lagrain, W. Boerjan, B. F. Sels, *Energy Environ. Sci.* **2015**, *8*, 1748–1763; d) W. Schutyser, S. Van den Bosch, T. Renders, T. De Boe, S. F. Koelewijn,

- A. Dewaele, T. Ennaert, O. Verkinderen, B. Goderis, C. M. Courtin, B. F. Sels, *Green Chem.* **2015**, *17*, 5035–5045; e) S. Van den Bosch, W. Schutyser, S. F. Koelwijjn, T. Renders, C. M. Courtin, B. Sels, *Chem. Commun.* **2015**, *51*, 13158–13161; f) M. V. Galkin and J. S. M. Samec, *ChemSusChem* **2014**, *7*, 2154–2158; g) T. Renders, W. Schutyser, S. Van den Bosch, S.-F. Koelwijjn, T. Vangeel, C. M. Courtin, B. F. Sels, *ACS Catal.* **2016**, *6*, 2055–2066.
- [9] C. Li, M. Zheng, A. Wang, T. Zhang, *Energy Environ. Sci.* **2012**, *5*, 6383–6390.
- [10] Q. Song, F. Wang, J. Cai, Y. Wang, J. Zhang, W. Yu, J. Xu, *Energy Environ. Sci.* **2013**, *6*, 994–1007.
- [11] a) I. Klein, B. Saha, M. M. Abu-Omar, *Catal. Sci. Technol.* **2015**, *5*, 3242–3245; b) H. Luo, I. M. Klein, Y. Jiang, H. Zhu, B. Liu, H. I. Kenttämä, M. M. Abu-Omar, *ACS Sustainable Chem. Eng.* **2016**, *4*, 2316–2322.
- [12] R. R. Fraser, M. Kaufman, P. Morand, G. Govil, *Can. J. Chem.* **1969**, *47*, 403–409.
- [13] Y. Zhao, D. G. Truhlar, *Theor. Chem. Acc.* **2008**, *120*, 215–241.
- [14] K. Lundquist, S. M. Li, V. Langer, *Acta Crystallogr. Sect. C* **2005**, *61*, o256–o258.
- [15] S. Kim, S. C. Chmely, M. R. Nimos, Y. J. Bomble, T. D. Foust, R. S. Paton, G. T. Beckham, *J. Phys. Chem. Lett.* **2011**, *2*, 2846–2852.
- [16] J. M. Younker, A. Beste, A. C. Buchanan, *ChemPhysChem* **2011**, *12*, 3556–3565.
- [17] H. Pines, T. P. Kobylinski, *J. Catal.* **1970**, *17*, 375–383.
- [18] H. Kim, J. Ralph, *Org. Biomol. Chem.* **2010**, *8*, 576–591.
- [19] a) M. Sette, R. Wechselberger, C. Crestini, *Chem. Eur. J.* **2011**, *17*, 9529–9535; b) F. P. Bouxin, A. McVeigh, F. Tran, N. J. Westwood, M. C. Jarvis, S. D. Jackson, *Green Chem.* **2015**, *17*, 1235–1242.
- [20] R. El Hage, N. Brosse, P. Sannigrahi, A. Ragauskas, *Polym. Degrad. Stab.* **2010**, *95*, 997–1003.
- [21] Gaussian 09, Revision D.01, M. J. Frisch, G. W. Trucks, H. B. Schlegel, G. E. Scuseria, M. A. Robb, J. R. Cheeseman, G. Scalmani, V. Barone, B. Menucci, G. A. Petersson, H. Nakatsuji, M. Caricato, X. Li, H. P. Hratchian, A. F. Izmaylov, J. Bloino, G. Zheng, J. L. Sonnenberg, M. Hada, M. Ehara, K. Toyota, R. Fukuda, J. Hasegawa, M. Ishida, T. Nakajima, Y. Honda, O. Kitao, H. Nakai, T. Vreven, J. A. Montgomery, Jr., J. E. Peralta, F. Ogliaro, M. Bearpark, J. J. Heyd, E. Brothers, K. N. Kudin, V. N. Staroverov, T. Keith, R. Kobayashi, J. Normand, K. Raghavachari, A. Rendell, J. C. Burant, S. S. Iyengar, J. Tomasi, M. Cossi, N. Rega, J. M. Millam, M. Klene, J. E. Knox, J. B. Cross, V. Bakken, C. Adamo, J. Jaramillo, R. Gomperts, R. E. Stratmann, O. Yazyev, A. J. Austin, R. Cammi, C. Pomelli, J. W. Ochterski, R. L. Martin, K. Morokuma, V. G. Zakrzewski, G. A. Voth, P. Salvador, J. J. Dannenberg, S. Dapprich, A. D. Daniels, O. Farkas, J. B. Foresman, J. V. Ortiz, J. Cioslowski, D. J. Fox, Gaussian, Inc., Wallingford CT, **2010**.

Received: September 12, 2016

Revised: October 12, 2016

Published online on ■ ■ ■, 0000





**Splitting wood:** High yield production of natural phenolic alcohols (38.7 wt%) from woody biomass has been achieved through an etherification–hydrogenolysis strategy. Using a Ni catalyst in a methanol–water co-solvent, we can

efficiently etherify the  $C_{\alpha}$ –OH group in lignin that can break the hydrogen bond ( $\text{OH}_{\alpha} \cdots \text{O}_{\beta}$ ) to facilitate the  $C_{\beta}$ –O cleavage, keeping the original structure of lignin unchanged.

*J. Chen, F. Lu,\* X. Si, X. Nie, J. Chen, R. Lu, J. Xu\**



**High Yield Production of Natural Phenolic Alcohols from Woody Biomass Using a Nickel-Based Catalyst**

